Recent applications and current trends in analytical chemistry using synchrotron-based Fourier-transform infrared microspectroscopy

Michael C. Martin, Ulrich Schade, Philippe Lerch, Paul Dumas

Synchrotron radiation based Fourier-transform infrared (SR-FTIR) microspectroscopy is an emerging technique, which is increasingly employed in analytical sciences. This technique combines FTIR spectroscopy (namely specific identification of molecular groups within a variety of environments: organic/inorganic, crystallized/amorphous, solid/liquid/gas) with high brightness, and therefore small spot size and faster acquisition of high-quality spectral imaging data from a synchrotron light source.

In this article, we review several recent applications of SR-FTIR that have led to much of the improved analytical capabilities. Performing analytical science at large-scale facilities allows one to access state-of-the-art equipment and capabilities, receive expert assistance from the facility staff, and have the possibility of combining SR-FTIR microscopy with other synchrotron-based X-ray microimaging techniques.

Keywords: Cultural heritage; Earth science; Fourier-transform infrared (FTIR); High pressure; Microspectroscopy; Polymer science; Space science; Synchrotron; X-ray; Vibrational linear dichroism

Michael C. Martin
Advanced Light Source Division, Lawrence Berkeley National Laboratory, 1 Cyclotron Road, B6R2100, Berkeley, CA 94720, USA

Ulrich Schade
Helmholtz Zentrum Berlin, BESSY II, Albert-Einstein-Strasse 15, 12489 Berlin, Germany

Philippe Lerch*
Swiss Light Source, Paul Scherrer Institut, 5232 Villigen, Switzerland

Paul Dumas
Synchrotron SOLEIL, L'Orme des Merisiers, BP48 - Saint Aubin, 91192 Gif-sur-Yvette Cedex, France

*Corresponding author.
Tel.: +41 56 310 3231;
E-mail: philippe.lerch@psi.ch

1. Introduction

The aim of this article is to discuss the new capabilities provided by synchrotron infrared (IR) beam-lines in the field of analytical chemistry. We illustrate with recent examples of applications in the fields of CH, space science, Earth science, biology, high pressure, and polymer science with vibrational linear dichroism. It was predicted years ago [1] that the IR emission from a synchrotron radiation (SR) source has potentially higher brilliance compared to a thermal source. However, it took more than a decade of development to harness the advantages of such sources. Modern IR spectroscopy uses the interference pattern of an IR beam split into two beams having a variable path-length difference (FTIR interferometry), typically sampled 10–100 times/ms, so the stability of the source on such a

0165-9936/$ - see front matter © 2010 Elsevier Ltd. All rights reserved. doi:10.1016/j.trac.2010.03.002

scale is of the utmost importance. Today, most SR facilities offer a port dedicated to IR spectroscopy and spectro-microscopy (Table 1). The high electron-beam stability of modern third-generation machines and the use of optical beam-stabilizing techniques [2] provide the required source stability for high-quality FTIR spectroscopy. The synchrotron source offers brightness (or brilliance or spectral radiance) 2–3 orders of magnitude higher than a thermal (laboratory-based) IR source [3,4], a high degree of polarization, as well as light pulses in the 2–10 ps time scale [5]. They are thoroughly exploited in the far-IR (FIR)/THz, and mid-IR (MIR) regions. In the long-wavelength domain, both flux and brightness exceed those of the thermal source [6].

The most rapidly expanding application of the synchrotron IR source is microspectroscopy on individual sample spots, as well as for chemical imaging. The principal advantages of the method are enhanced lateral resolution (typically at or very close to the diffraction limit [7,8] combined with superior signal-to-noise ratio obtained without resorting to prohibitively long acquisition times. These advantages have been widely exploited in synchrotron facilities worldwide. Numerous achievements in a variety of scientific disciplines (e.g., soft matter [9,10], geology [11–13], biology [14–23], environmental science [24,25]) have been reported. The increasing demand for beam time, as well the potential for impact in fields such as analytical chemistry, has triggered the construction of more synchrotron IR beam lines worldwide (Table 1).

IR-microscopy imaging makes use of the rich, unique spectroscopic absorption features found in the MIR spectral region for chemical identification to form images based on these absorption bands. However, there is increasing interest in extending the spectral range to lower frequencies. This trend is motivated by developments in coherent THz spectroscopy and imaging [26] as well as by the need of the space-sciences community to identify complex minerals found in interplanetary dust particles [27]. The broad spectral coverage and high brightness of SR reaches well into the FIR, to below 1 THz and coherent SR has the potential to be an exciting powerful THz source [28,29].

Basic work has been done at BESSY II [30] to make this coherent broadband THz source accessible to spectroscopic applications at storage rings for not only conventional spectroscopic techniques [31–34] but also near-field spectral imaging on biological samples in the THz range [35,36]. The purpose of this review article is to illustrate how synchrotron IR emission has advanced IR microspectroscopy and imaging in analytical

Table 1. Facilities that plan (P) or operate (O) mid-IR beam-lines. List: http://infrared.als.lbl.gov/content/web-links/45-srir

Facility	Location	Beamline	URL
ALBA	Barcelona, Spain	1 P	www.cells.es/Beamlines/SECOND-PHASE/MIRAS/
ALS	Berkeley, USA	2 O, 1 P	infrared.als.lbl.gov/
ANKA	Karlsruhe, Germany	2 O	ankaweb.fzk.de/website.php?page=instrumentation_beam&id=1
Australian Synchrotron	Melbourne Australia	1 O	www.synchrotron.org.au/index.php/aussyncbeamlines/infrared-micro/beamline-team
BESSY II	Berlin, Germany	1 O	www.helmholtz-berlin.de/
CAMD	Baton Rouge, USA	1 O	www.camd.lsu.edu/pdf/NIMA-IR.pdf
CLS	Saskatoon, Canada	2 O	www.lightsource.ca/experimental/midir.php
DAFNE	Frascati, Italy	1 O	www.lnf.infn.it/
Diamond	Oxfordshire, UK	1 O	www.diamond.ac.uk/Home/Beamlines/B22.html
Elettra	Trieste, Italy	1 O	www.elettra.trieste.it/experiments/beamlines/sissi/
ESRF	Grenoble, France	1 O	not accessible as general User instrument
INDUS-1	Indore, India	1 P	www.cat.ernet.in/index.html
Jlab	Newport News, USA	1 O	www.jlab.org/FEL/terahertz/
MAX-lab	Lund, Sweden	1 O	www.maxlab.lu.se/beamlines/bl73/
Metrology LS	Berlin, Germany	2 O	www.ptb.de/mls/
NSLS	Brookhaven, USA	6 O	infrared.nsls.bnl.gov/
NSRL	Hefei, China	1 O	www.nsrl.ustc.edu.cn/EN/
NSRRC	Hsinchu, Taiwan	1 O	www.nsrrc.org.tw/lifensrrc/bl14a1.htm
SESAME	Allan, Jordan	1 P	www.sesame.org.jo/About/Beam.aspx
Siam PS Photon Source	Nakhon Ratchasima Thailand	1 P	www.slri.or.th/new_eng/index.php?option=com_content&task=view&id=52&Itemid=89
SLS	Villigen, Switzerland	1 O	sls.web.psi.ch/view.php/beamlines/ir/index.html
SOLEIL	Gif-sur-Yvette France	2 O	www.synchrotron-soleil.fr/portal/page/portal/Recherche/LignesLumiere/SMIS
SPring-8	Hyogo, Japan	1 O	infrared43.spring8.or.jp
SRC	Madison, USA	2 O	www.src.wisc.edu/facility/complist.htm
SSLS	Singapore	1 O	ssls.uus.edu.sg/facility/facility.htm
SSRF	Shanghai, China	1 P	ssrf.sinap.ac.cn/english/
UVSOR	Okazaki, Japan	1 O	www.uvsor.ims.ac.jp/inforuvsor/beamlines.pdf

chemistry in ways that would prove quite difficult with a conventional thermal IR source. In the following, we introduce briefly the synchrotron IR source, its power, its brightness (spectral radiance or brilliance), its intensity distribution at the detector as well as its wavelength dependence. We illustrate, with selected examples, how these source properties have been exploited in analytical chemistry.

2. Synchrotron IR source

Electron-based synchrotron light sources use magnetic fields to bend the electron trajectory into a closed orbit. SR is produced at each of these bending magnets. The emitted radiation spans an extremely broad spectral domain, extending from the X-ray regime to the very FIR region. IR radiation is generated by electrons traveling at relativistic velocities, either along a curved path through a constant magnetic field {i.e. bending magnet (BM) radiation [1]} or when their trajectories encounter variable magnetic fields, e.g., at the edges of BM {i.e. edge radiation [37,38]}. The SR from the constant magnetic field provides circularly polarized light, left-handed and right-handed for the radiation extracted above and below the storage-ring plane, respectively. The degree of polarization depends on the details of the radiation-extraction scheme. Some experiments require a high degree of linear polarized light (e.g., see Section 6). By contrast, the edge radiation is radially linearly polarized.

Flux and brightness for the two types of IR emission are almost equivalent, but the opening angle of the ER is narrower than that of the SR from constant field of a BM [39,40]. The crucial parameter here is the effective size of the synchrotron source. For newer storage rings, it is of the order of 100 μm or less, so light is emitted into a narrow range of angles and the resulting brightness is increased by 2–3 orders of magnitude above the brightness of a thermal source [40]. An SR X-ray source offers more flux than a regular laboratory source. In the MIR energy range, this is no longer true. In fact, the total MIR flux emitted from a thermal source can be 1–2 orders of magnitude lower than the flux emitted by an SR source. This trend is inversed at longer wavelengths [41].

In microscopy, the spatial resolution of SR-FTIR is usually only limited by the wavelength, λ, of IR light [42], which is longer than for visible light used for optical microscopy. Typical Schwarzschild objectives have a numerical aperture in the range 0.5–0.6. Some microscopes use a single aperture placed before light reaches the sample, which defines the illuminated sample region. In such a situation, the diffraction-limited spatial resolution is approximately [7] $2\lambda/3$ which corresponds to 1.7 μm (at 4000 cm^{-1}) and 13 μm (at 500 cm^{-1}).

Other microscopes operate in the so-called confocal arrangement, where a second aperture is placed so as to limit light collection to the region of interest of the sample. In this geometry, the two apertures are placed in conjugates planes of the two IR objectives. This method, discussed by G.L. Carr [7,40], improves spatial resolution to $\lambda/2$. In addition, the confocal arrangement also reduces the Schwarzschild's first-order and higher-order diffraction rings, resulting in improved image contrast [7]. More details about instrument and beam-line characteristics are available [39,40].

3. Applications in the field of cultural heritage

FTIR and Raman spectroscopy are two methods well suited to the study of ancient compounds [41]. These two vibrational techniques are becoming popular in museums and their associated scientific institutions. Raman microscopy uses laser excitation, possibly inducing damage to often rather precious samples, but FTIR microscopy can be used safely on cultural heritage (CH) samples. The life-science community was first to lead the demand for analysis at the diffraction limit made possible by SR-FTIR microscopes [16,42]. Today, CH scientists realize the benefits of improved data quality, signal-to-noise ratio, dwell time and lateral resolution offered by SR.

Samples are often complex mixtures of organic and inorganic compounds at the μm scale. Two factors are responsible for the important contributions of SR-IR microscopy in this field. First, the brightness advantage allows us to obtain high-quality spectra regardless of the roughness and the heterogeneity of the micro fragments. High brightness allows us to compensate for some of the restrictions imposed in sample preparation due to the unique origins of samples. Second, raster scanning the sample allows us to generate 2D maps of distributions of molecular groups (chemical images), which can be correlated with conventional images to reveal the morphology.

Following the seminal article by G.D. Smith [43], the number of studies including SR-FTIR has increased. Some studies focused on the identification of organic compounds {e.g., resinous materials used to seal ancient Roman or Iberian amphorae [44], organic coatings on historical 18th and 19th century furniture [45], and corrosion compounds on bronze objects [46]}. Recently, there have been reports of simultaneous identification of organic materials (binders, mordants, varnishes, glazes, pigments) and inorganic materials (pigments, filler) together with hybrid materials (e.g., carboxylates) that result from the reaction of organic and inorganic compounds [47–50]. Complex hybrid formulations (e.g., those found in ancient cosmetics [51], the patina of African statues [52], or the varnish covering ancient

musical instruments [53,54]) can readily be investigated by SR-IR microspectroscopy. In all these cases, the sample complexity reflects the methods and the choices of the artist and the craftsman as well as the reactions involved in the alterations. The ability to identify, at the μm scale, the majority of these constituents is a clear asset, as more precise knowledge of ancient formulation practices and some of the subsequent degradation phenomena can the be obtained.

With SR-FTIR microspectroscopy, it is possible to image characteristic structures of prehistoric bone [e.g., the osteons (the constitutive histological unit of cortical bone) using the absorption-band ratios corresponding to different chemical constituents of bone (e.g., collagen content and quality, phosphate crystallinity, and carbonate content)]. Reiche et al. used this approach to evaluate, at a histological level [55], the state of preservation of a 5000-year-old bone found at the Neolithic site of Chalain lake.

In ancient biological tissues, for example, the heterogeneity is intrinsic to the sample. Alterations, as well as possible biomineralization, which produce hybrid materials, might modify or even increase the complexity of the chemical composition. Comparison between fresh and ancient tissues enables us to identify decay markers. With 2D chemical imaging, these markers can be located across the whole tissue structure (e.g., showing that, for skin, the outmost layers are far from being the most degraded [56]). Fig. 1 illustrates the chemical imaging analysis of a wall-painting fragment discovered in cave N(a), on the Bamiyan site, Afghanistan, in the context of a wide conservation project dedicated to Buddhist painting techniques from 5th–9th centuries, funded by the UNESCO/Japanese Funds-in-Trust [57]. These paintings of complex chemical composition revealed sophisticated ancient technology. The study identified a wide palette of pigments and organic materials that were mixed and coated in multi-layers, leading to refined optical effects. The identification of oil in particular sheds entire new light on the historical development of oil painting techniques [50,58].

Fig. 1A shows the sample structure: 1 = yellowish transparent layer, 2 = green layer, 3 = black layer, 4 = white ground, 5 = transparent brownish layer, and

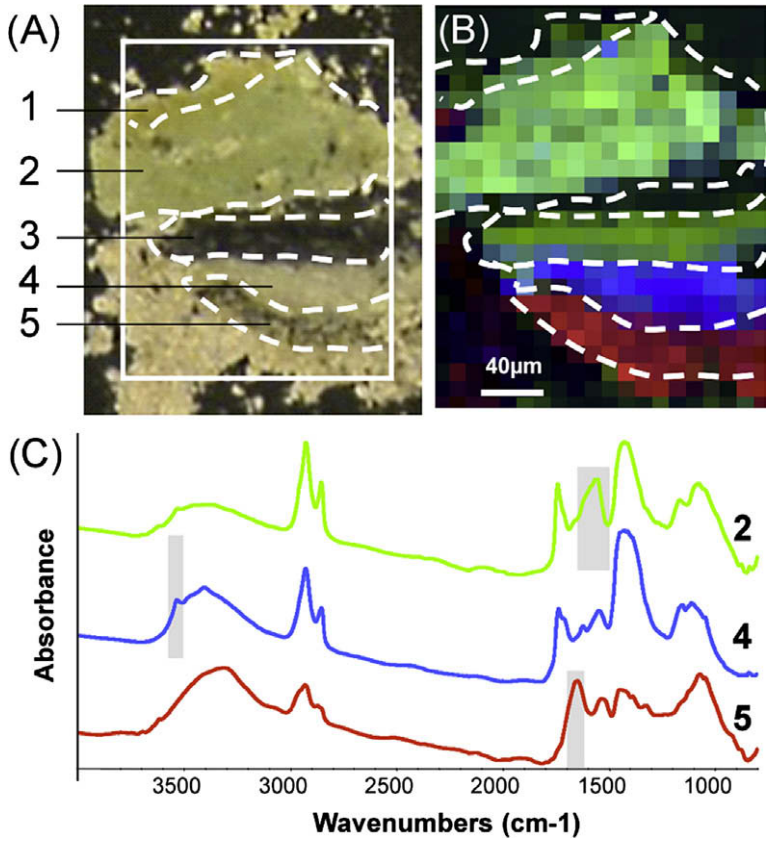

Figure 1. A) Photomicrograph of pressed fragment of sample BMM035 from Cave N(a), Bamiyan, showing a multi-layered structure: 1 = yellowish transparent layer, 2 = green layer, 3 = black layer, 4 = white ground, 5 = transparent brownish layer, and earthen rendering. B) Chemical mappings obtained by SR-μFTIR, showing the distribution of three particular ingredients: in red, proteins; in green, carboxylates; in blue, hydrocerussite. Map size: 190 × 170 μm; step size : 10 × 10 μm. C) Average FTIR spectra obtained in the green layer (2), the white ground layer (4) and the transparent brownish layer (5). The grey rectangles highlight the vibrational bands used to generate chemical mappings displayed in B). (Reproduced from [60] with permission).

earthen rendering. The complete study is detailed elsewhere [59]. Average spectra obtained in layers 2, 4 and 5 are shown in Fig. 1C. Fig. 1B presents the chemical map of three ingredients identified (1 organic, 1 hybrid, and 1 inorganic) and localized by SR-FTIR. In red, the protein-based sizing/sealing (probed by the characteristic amide I band, at 1650 cm^{-1}), restricted to layer 5. It can indicate the use of either egg white or animal glue. In green, carboxylates (probed by the C═O stretching around 1550 cm^{-1}), resulting from the reaction of oil esters with some inorganic compounds. In this case, a mixture of lead and copper soaps is suspected, particularly in the green layer. In blue, hydrocerussite ($Pb_3(CO_3)_2(OH)_2$), is identified by the characteristic OH stretching at 3534 cm^{-1}. This lead carbonate enters into the composition of lead white. It is highly concentrated in the white layer (4), but detected in the green layer (2). Various components, being inorganic, organic or hybrid materials, can be identified and located across the complex morphology of the sample with a rather good lateral resolution (10 μm here). This level of sample complexity and heterogeneity is typical of paintings and more generally in artwork.

4. Chemistry and polymer application of SR-IR

In recent years, numerous in-situ microspectroscopic techniques have been explored to investigate catalytic reactions occurring in heterogeneous catalysts using time and space domain-resolved approaches. However, this requires the study of catalytic reaction in situ, within zeolite grains or crystals. Recently, E. Stavitski et al. [61] were the first to demonstrate, through the study of H-ZSM-5 microcrystals exposed to 4-fluorostyrene both by point spectroscopy and imaging, that such in situ exploration is feasible using SR-IR microscopy and should open new avenues for such a research field.

Despite the fact that IR spectroscopy is the most widely-used technique for the characterization of polymers, providing a rich source of information on diverse aspects from the composition of polymeric materials to the molecular configuration, conformation and orientational properties of polymer chains, very few studies have been performed using SR-IR microspectroscopy. However, it is an important domain of application, as evidenced by the work of Ellis and co-workers in micropatterned biodegradable copolymers, oriented semicrystalline polymers and multilayered materials [9,62,63].

5. Live biochemical processes studied by SR-IR

Real-time chemical imaging of cellular and bacterial activities can facilitate comprehensive understanding of the dynamics of structures and functions of various living systems from human cells to biofilms in the environment. SR-FTIR spectromicroscopy can yield high spatial resolution and label-free vibrational signatures of chemical bonds in biomolecules, but the abundance of water in most biofilms and tissues has hindered SR-FTIR sensitivity in investigating bacterial activity.

An open-channel microfluidic system was employed by Holman et al. [22] to circumvent the water-absorption barrier for chemical imaging of the developmental dynamics of bacterial biofilms with a spatial resolution of several μm. This system maintains a 10-μm thick laminar-flow-through biofilm system that minimizes both the imaging volume in liquid and the signal interference from geometry-induced fringing. The open-channel microfluidic platform maintains the functionality of living cells while enabling high-quality SR-FTIR measurements having multiple-molecule sensitivity with μm spatial resolution. The ability to monitor and to map bacterial changes in biofilms directly can yield significant insight into a wide range of microbial systems, especially when coupled to more sophisticated microfluidic platforms. This might then be used to investigate many important microbial systems, including harmful processes (e.g., chronic bacterial infections) or beneficial processes (e.g., energy production in microbial fuel cells).

SR-FTIR microspectroscopy can also be employed for label-free and time-resolved monitoring of rapid biochemical reactions. Kaun et al. [64] used a lab-on-a-chip device made of CaF_2 windows and SU-8 polymer to achieve rapid mixing of two streamlines with a cross-section of 300 μm width × 5 μm cell depth. Time-resolved measurements of the induced chemical reaction in strongly absorbing water solutions are achieved by applying constant flow rates and by on-chip measurement at defined distances after the mixing point. Kaun and co-workers [64] studied the interaction between the antibiotic vancomycin and a tripeptide (Ac2KAA), which is involved in the build-up of the membrane proteins of gram-positive bacteria. The diffraction-limited spot size of the IR SR, using a 32× objective for the microscope, sets the time resolution of their experimental set-up down to 500 μs.

With the completion of sequencing of genomes of many organisms and the success in identifying gene products (proteins) and metabolic pathways, one of the central interests in biogeochemical and environmental research is to apply this wealth of information to understand and to design appropriate strategies to utilize metabolic capabilities in living microorganisms to remediate pollutants in earth and environmental materials. Success will ultimately be determined by how well one can measure without disturbing the relevant dynamic processes in a biogeochemical system (e.g., the redox transformations of heavy metals by metal-reducing bacteria, or degradation of carcinogenic

organic pollutants). SR-FTIR spectromicroscopy was successfully used to determine that certain bacteria found naturally in basalt are effective agents in the ''biogeochemical'' transformation of chromium from the undesirable hexavelant state to the less harmful trivalent state, thereby resolving an on-going controversy about the nature of the conversion [65]. The technique has also been used to show that the speed of biodegradation of polycyclic aromatic hydrocarbons (PAHs) can be dramatically increased (by almost 100-fold) by adding soil-derived humic acid along with mycobacteria on a mineral surface [25]. These results suggest that someday it may be routine to study a tiny microbial colony, by using SR-IR spectroscopy, and to screen for microbes and conditions that are most effective in detoxifying environmental pollutants [12].

6. Microspectroscopic studies of vibrational linear dichroism using polarization-modulated SR-IR

Oriented samples absorbing in the IR wavelength range show differential absorption between orthogonal states of linearly polarized radiation [i.e. they exhibit vibrational linear dichroism (VLD)]. The spectral information obtained from VLD studies links the spatial arrangement of sub-molecular structures and functional groups to macroscopic material properties. The combination of the polarization-modulation technique with FTIR spectroscopy provides a sensitive method to study VLD [66]. The technique is based on a photoelastic modulator (PEM) modulating the polarization of the IR radiation at a high frequency and delivers a reference-free spectrum directly related to the dichroic difference spectrum. Moreover, by combining it with an IR microscope and applying IR SR, the characterization of molecular orientation and the quantification of anisotropy as well as order and disorder in matter can be performed with a spatial resolution down to the diffraction limit. Polarization-modulated (PM) SR-IR microspectroscopy has been widely applied at BESSY II in recent years [66–68] and will soon be available at the Canadian Light Source.

Schmidt et al. applied PM SR-IR microspectroscopy to investigate hydrogen bonding in wood polymers [66]. They used mechanically-isolated single-spruce fibers and studied the polymers in their native composite structure. The fibers were placed in a microfluidic cuvette and exposed to different solvents. In contrast to normal absorption measurements, here only the spruce fiber itself contributed to the spectrum since the bulk solvents were isotropic. In particular, Schmidt et al. observed differences in the O–H stretching region of the VLD spectra upon changing the ambient condition of the fiber (see Fig. 2) and derived from these changes information on the hydrogen bonding as well as on how structural units of the wood polymers in the spruce cell walls were accessible and how they were oriented.

It has been demonstrated that PM SR-IR microspectroscopy is also applicable for reflection difference (PM-RD) studies of solid-state samples [67–69]. Exploiting the high brilliance of SR-IR together with the mapping capability of the confocal IR microscope, anisotropic domains in $Bi_{0.17}Ca_{0.83}MnO_3^+$ were imaged. In this particular sample, the domains that had different optical axes were inhomogeneously distributed within tens of μm (see Fig. 3). Furthermore, optical anisotropy of a

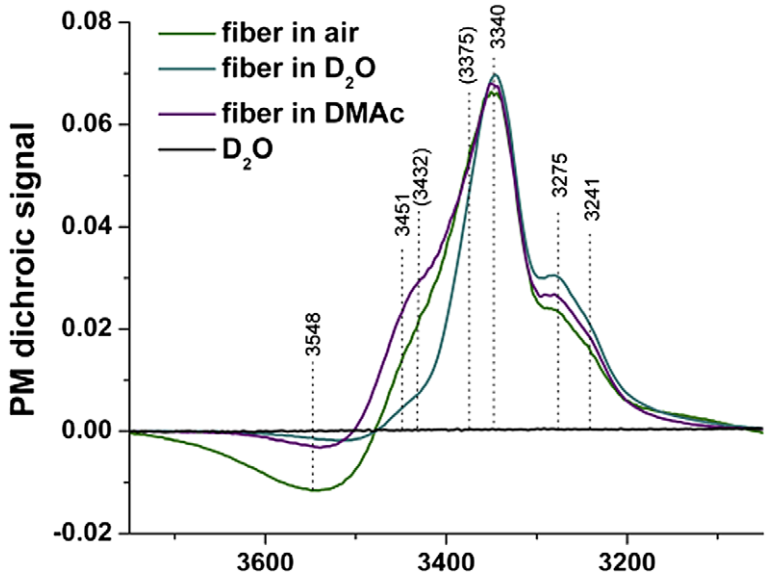

Figure 2. Polarization-modulated dichroic spruce fiber spectra (each an average of three single fibers measurements) recorded in air, D_2O, and dimethylacetamide (DMAc), and a background (D_2O in the microfluidic cuvette) spectrum as control.

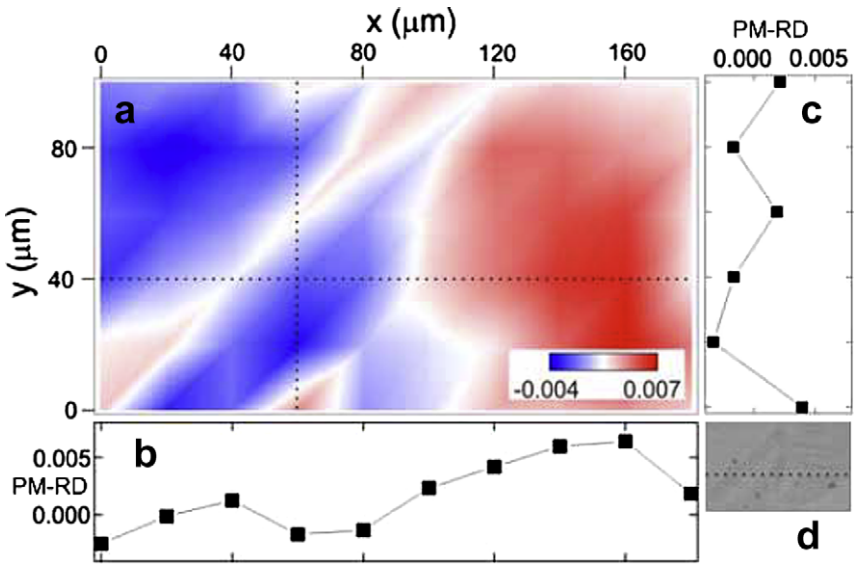

Figure 3. a) Spatial distribution of the PM-RD signal of the $Bi_{0.17}Ca_{0.83}MnO_{3+\delta}$ crystal at 4000 cm^{-1} for the given area shown as a visible image in d). b) and c) Line profiles of the signal along the dotted lines indicated in a). d) Visible image of the sample area investigated.

$Bi_{0.17}Ca_{0.83}MnO_{3+\delta}$ crystal induced by charge and orbital orderings was investigated. PM-RD spectra of local domains were acquired as a function of azimuthal angle and temperature. Besides a drastic change in the anisotropic response below the charge ordering transition around 16°C, an additional change in the optical anisotropy was observed at a slightly lower temperature close to 13°C. This intriguing change, accompanied by a 45° rotation of the optical axis, was claimed to be the signature of orbital ordering that did not coincide with the charge-ordering transition observed with decreasing temperature [67].

7. High-pressure studies

Exploring the properties of matter beyond usual room temperature, pressure, (and/or magnetic field) allows us to survey complex phase diagrams and to study substances in environments (e.g., those present at high pressure within the mantle of a planet). Having analytical chemistry in mind, ''pressure'' can be thought as a ''dial'', by which the strength of some molecular interactions can be varied by several orders of magnitude while monitoring their IR response. Samples mounted in a diamond anvil cell (DAC) can well be investigated using (IR and X-ray) synchrotron light, since the diameter defined by the gasket of the DAC nicely matches the spot size of the SR source.

Several disciplines benefit from high-pressure studies (e.g., molecular crystals [70], hydrogen-rich solids [71] and related planetary materials, minerals of the Earth's crust, mantle, and core [72], glasses and melts [73], whole-rock samples [74,75], novel high-pressure materials of technological interest [76], and pioneering studies of pressure-induced phase transitions in oxides and strongly correlated systems [77,78]). For example, the water content in minerals localized in the (pressurized) mantle transition zone of the Earth affects several physical properties (e.g., molar volume, thermal expansion, elastic moduli, and heat transfer). Water is likely to affect the mantle dynamics, so the interpretation of seismic data directly benefits from enhanced knowledge on the impact of water. High-pressure IR studies on phase transformations in $(Mg,Fe)_2SiO_4$ from olivine to wadsleyite and wadsleyite to ringwoodite, respectively, increase our knowledge on the discontinuity of the p-wave and s-wave velocities at depths of 410 km and 520 km in the Earth's mantle. Chamorro-Pérez et al. [75] studied hydrous Mg-ringwoodite (1 and 1.7 wt /100 water) under high pressure with SR microspectroscopy up to 30 GPa. They observed a second-order phase transition close to 25 GPa, revealed by a sudden disappearance of the OH band near 3150 cm^{-1}.

In order to further investigate the role of pressure on the local arrangement of hydrogen in iron-rich $(Fe,Mg)_2SiO_4$ samples, Koch-Müller et al. [79] synthesized hydrous ringwoodite with concentrations in the range $x_{Mg} = 0–0.61$. IR spectra collected at different pressures up to 30 GPa using three different pressure-transmitting environments suggested that the transition observed in hydrous Mg-ringwoodite endmember is absent in material containing Fe. By comparing the

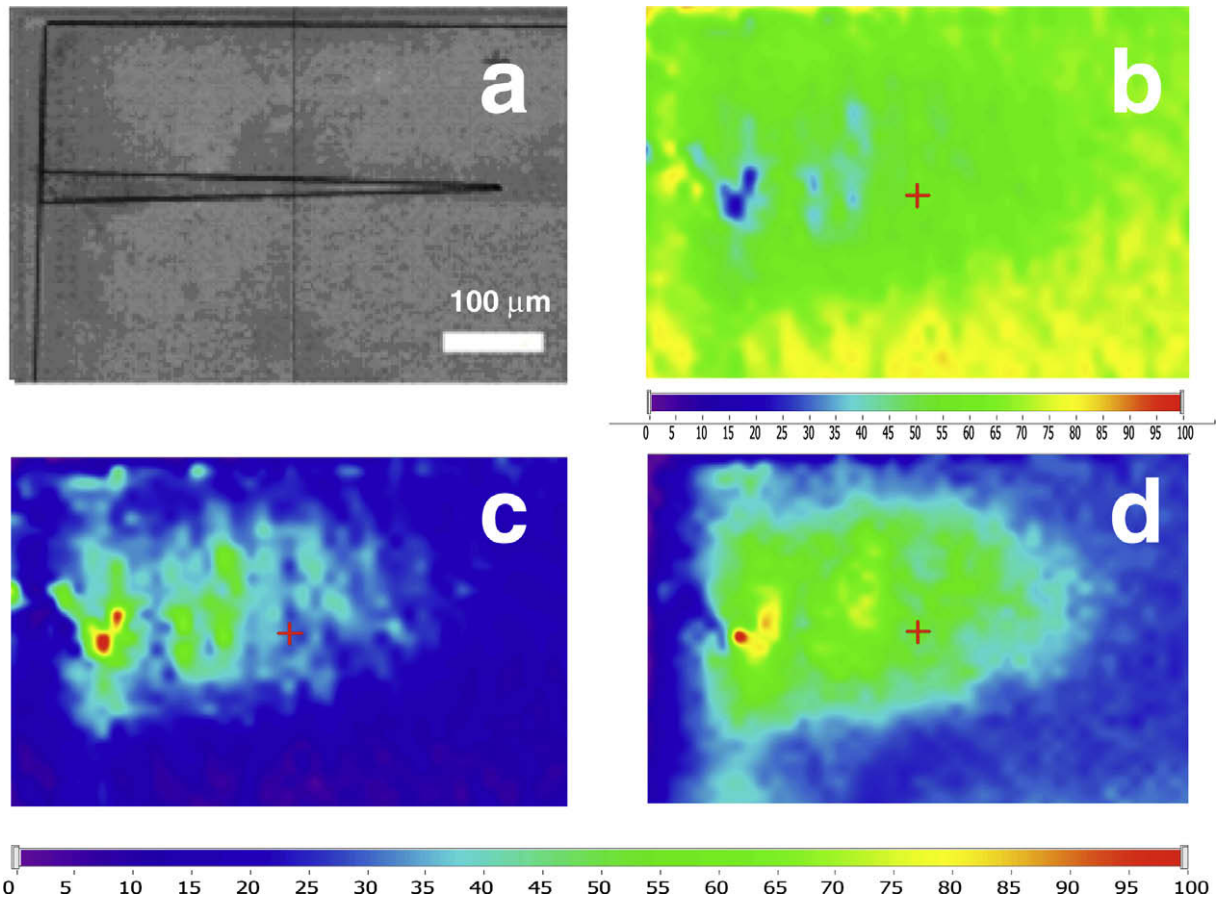

Figure 4. a) Optical image showing the edges of the keystone and the approximate outline of the STARDUST track C2009,7,62. The original surface exposed to the comet is on the left. b) Raw transmission map for 2926 wavenumbers. The color scale is 0–100%T. c) Absorbance map for the same spectral wavenumber position as b). d) Background corrected absorbance map for the aforementioned wave number. c) and d) have the same scale 0–100% absorbance. The 100-μm bar in a) gives the dimensional scale for all four images. (Adapted from [83]).

behavior of samples compressed in various environments, they argued that the sudden disappearance of the OH band in hydrous ringwoodite was more likely to have been driven by the deterioration of the quasihydrostatic stress condition than by a pressure-induced effect.

Additional questions of interest arise in the FIR/THz region, as with increasing radiation wavelength, the in-situ DAC experiments would require an aperture of at least 1 mm to overcome the intensity loss of conventional sources due to diffraction. Such a large aperture limits the maximum pressure to about 1 GPa. However, the FIR region provides important structural information at high pressures, at which the metal cations are involved on vibrational absorptions. In order to address this topic, a vacuum FIR/THz microscope utilizing SR IR was developed operating down to 300 μm (1 THz) for apertures of the DAC of 300 μm. First results on pressure-induced structural changes in silicate minerals (e.g., feldspar, olivine and wadsleyite) have been obtained for high pressures up to 20 GPa [80].

8. Space-science samples

IR spectroscopy is the primary means of mineralogical analysis of materials collected from space. The identity and the properties of grains are inferred from spectral comparisons between astronomical observations and laboratory data from natural and synthetic materials [81]. Among important studies, that of the Stardust mission is briefly reported here. The Stardust mission flew through the near-nucleus coma of comet 81P/Wild 2 on 2 January 2004, swept up material using aerogel collectors, and returned these samples to Earth on 15 January 2006. Stardust is the first space mission to bring back solid material from a known body other than the Moon. A special issue of *Science* in December 2006 summarized the main findings of the Preliminary Examination Team. One discovery made by synchrotron IR microspectroscopy was the distribution of volatile organic components in and around the particle tracks [82,83] as shown in Fig. 4.

When particle tracks contained volatile organic material, they were found to be $–CH_2$-rich, while the aerogel is dominated by the $–CH_3$-rich contaminant. It is clear that the population of cometary particles impacting the Stardust aerogel collectors also included grains that contained little or none of this organic component. This observation is consistent with the highly heterogeneous nature of collected grains, as seen by a multitude of other analytical techniques.

Other meteoritic samples have also been studied by SR FTIR. The mineralogical and chemical composition of the meteorites Dho 225 and Dho 735 recently found in Oman suggested that these unusual meteorites were thermally metamorphosed CM2 chondrites. Similar to Antarctic metamorphosed carbonaceous chondrites, these newly found meteorites were enriched in heavy oxygen compared to normal CMs. Non-destructive SR-IR microspectroscopy studies of these precious samples from outer space indicated that the two new meteorites from Oman were the first non-Antarctic thermally-metamorphosed carbonaceous chondrites under study so far [81].

9. Summary

Microanalytical studies are actively pursued at synchrotron facilities. The general SR beam-time requests for experiments in analytical chemistry are increasing worldwide. Many researchers are already using conventional IR microscopes, equipped either with a single detector or pixel-array detectors. The synchrotron source provides improved spectral quality (signal-to-noise) and higher lateral resolution. Today, efforts dedicated to improve the stability of the e-beam in storage rings, and to minimize residual noise sources in the beam-line design, result in very stable SR-IR sources. The high brightness can be exploited for very efficient analysis. One limitation is set by the diffraction-limited spot size. The use of pixel-array detectors combined with sophisticated signal treatment has recently been suggested [40]. This route will benefit from the increase in IR flux possible with very large BM horizontal collection angle.

Near-field methods allow us to break the ''diffraction limit'' [35,84,85]. Efforts devoted to broadband nearfield IR microscopy using the SR source could result in lateral resolution of $\lambda/10$ or better. Such a breakthrough has yet to be reported. The THz energy range, more commonly called FIR, might benefit from the coherent SR produced when relativistic electron bunches have longitudinal density variations on a scale comparable to or smaller than the wavelength. Synchrotron and transition radiation emitted from a bunched electron beam becomes coherent and highly intense at wavelengths about or longer than the bunch length. This radiation has a continuous spectrum in the sub-mm to mm wavelength range.

Raman microscopy is a widespread vibrational spectroscopy method. It offers equivalent or even better spatial resolution than SR-IR microscopy, but suffers from potential radiation damages, as well as fluorescence emission. For some samples, difficulties with absorption and fluorescence can lower the spectral quality. However, the two methods are very complementary and should become available at SR facilities.

One of the most promising avenues, which is starting to be exploited in synchrotron facilities, is the unique opportunity to combine IR microscopy with other synchrotron-based techniques. The strategy for efficient combination relies upon the choice of adequate substrate and sample holder, and good coordination between beam-time allocations on different end stations. Such combined approaches will greatly benefit analytical chemistry.

Acknowledgments

The authors are grateful to F. Jamme and C. Sandt (SOLEIL), M. Cotte and J. Susni (ESRF), G.L. Carr and L.M. Miller (NSLS), G.P. Williams (Jefferson Labs), H.-Y. Holman and W.R. McKinney (LBNL) for their long-term collaborations and fruitful discussions. The Advanced Light Source is supported by the Director, Office of Science, Office of Basic Energy Sciences, US Department of Energy under Contract No. DE-AC02-05CH11231.

References

[1] W. Duncan, G.P. Williams, Appl. Opt. 22 (1983) 2914.
[2] T. Scarvie, N. Andreson, K. Baptiste, J.M. Byrd, M.J. Chin, M.C. Martin, W.R. McKinney, C. Steier, Infrared Phys. Technol. 45 (2004) 403.
[3] G.L. Carr, J.A. Reffner, G.P. Williams, Rev. Sci. Instrum. 66 (1995) 1490.
[4] W.R. McKinney, C. Hirschmug, H. Padmore, T. Lauritzen, N. Andreson, G. Andronaco, R. Patton, M. Fong, SPIE Proc 3153 (1997) 59.
[5] R.P.S.M. Lobo, J.D. LaVeigne, D.H. Reitze, D.B. Tanner, G.L. Carr, Rev. Sci. Instrum. 73 (2002) 1.
[6] R.P.S.M. Lobo, J.D. LaVeigne, D.H. Reitze, D.B. Tanner, G.L. Carr, Rev. Sci. Instrum. 70 (1999) 2899.
[7] G.L. Carr, Rev. Sci. Instrum. 72 (2001) 1613–1619.
[8] E. Levenson, P. Lerch, M.C. Martin, J. Synchrotron Radiat. 15 (2008) 323.
[9] G. Ellis, C. Marco, M. Gómez, Infrared Phys. Technol. 45 (2004) 349.
[10] G. Ellis, C. Marco, M.A. Gómez, E.P. Collar, J. Ma. García-Martínez, J. Macromol. Sci., B Phys. 43 (2004) 253.
[11] N. Guilhaumou, P. Dumas, G.L. Carr, G.P. Williams, Appl. Spectrosc. 52 (1998) 1029.
[12] H.-Y.N. Holman, M.C. Martin, Adv. Agronomy 90 (2006) 79.
[13] J. Watkins, M. Manga, C. Huber, M.C. Martin, Contributions Mineral. Petrol. 157 (2009) 163.
[14] P. Dumas, L. Miller, J. Biol. Phys. 29 (2003) 201.
[15] P. Dumas, L. Miller, Vib. Spectrosc. 32 (2003) 3.
[16] P. Dumas, G.D. Sockalingum, J. Sulé-Suso, Trends Biotechnol. 25 (2007) 40.

[17] L.M. Miller, G.L. Carr, M. Jackson, P. Dumas, G.P. Williams, Synchrotron. Radiat. News 13 (2000) 31.
[18] L.M. Miller, P. Dumas, N. Jamin, J.L. Teillaud, J.L. Bantignies, G.L. Carr, Microbeam Anal. Proc., Inst. Phys. Conf. Ser. 165 (2000) 75–76.
[19] L.M. Miller, R. Huang, M.R. Chance, C.S. Carlson, Synchrotron. Radiat. News 12 (1999) 21.
[20] H.-Y.N. Holman, M.C. Martin, W.R. McKinney, Spectrosc.– Int. J. 17 (2003) 139.
[21] H.-Y.N. Holman, E. Wozei, Z. Lin, L.R. Comolli, D.A. Ball, S.C. Borglin, M.W. Fields, T.C. Hazen, K.H. Downing, Proc. Natl. Acad. Sci. USA 106 (2009) 12599.
[22] H.-Y.N. Holman, R. Miles, Z. Hao, E. Wozei, L.M. Anderson, H. Yang, Anal. Chem. 81 (2009) 8564.
[23] H.-Y.N. Holman, K. Bjornstad, M.C. Martin, W.R. McKinney, E.A. Blakely, F.G. Blankenberg, J. Biomed. Opt. 13 (2008) 030503.
[24] H.-Y.N. Holman, K. Nieman, D.L. Sorensen, C.D. Miller, M.C. Martin, T. Borch, W.R. McKinney, R.C. Sims, Environ. Sci. Technol. 36 (2002) 1276.
[25] C. Hirschmugl, Rev. Mineral. Geochem. 49 (2002) 317.
[26] D.M. Mittleman, R.H. Jacobsen, M.C. Nuss, IEEE J. Sel. Top. Quantum Electron. 2 (1996) 679.
[27] L.P. Keller, S. Hony, J.P. Bradley, F.J. Molster, L.B.F.M. Waters, J. Bouwman, A. de Koter, D.E. Brownlee, G.J. Flynn, T. Henning, H. Mutschke, Nature (London) 417 (2002) 148.
[28] G.L. Carr, M.C. Martin, W.R. McKinney, K. Jordan, G.R. Neil, G.P. Williams, Nature (London) 420 (2002) 153.
[29] S. Bielawski, C. Evain, T.M. Hara, M. Katoh, S. Kimura, A. Mochihashi, M. Shimada, C. Szwaj, T. Takahashi, Y. Takashima, Nature (London) Phys. Sci. 4 (2008) 390.
[30] M. Abo-Bakr, J. Feikes, K. Holldack, H.-W. Hübers, P. Kuske, W.B. Peatman, U. Schade, G. Wüstefeld, Phys. Rev. Lett. 90 (2003) 094801.
[31] E.J. Singley, M. Abo-Bakr, D.N. Basov, J. Feikes, P. Guptasarma, K. Holldack, H.W. Hübers, P. Kuske, M.C. Martin, W.B. Peatman, U. Schade, G. Wüstefeld, Phys. Rev. B. 69 (2004) 092512.
[32] D.N. Basov, J. Feikes, K. Holldack, H.-W. Hübers, P. Kuske, M.C. Martin, S.G. Pavlov, U. Schade, E.J. Singley, G. Wüstefeld, ICFA Beam Dynamics Newsletter 35 (2004) 57.
[33] M. Ortolani, S. Lupi, L. Baldassarre, P. Calvani, U. Schade, Y. Takano, M. Nagao, T. Takenouchi, H. Kawarada, Phys. Rev. Lett. 97 (2006) 097002.
[34] U. Schade, M. Ortolani, J.S. Lee, Synchrotron Radiat. News 20 (2007) 17.
[35] U. Schade, K. Holldack, P. Kuste, G. Wüstefeld, H.-W. Hübers, Appl. Phys. Lett. 84 (2004) 1422.
[36] U. Schade, K. Holldack, M.C. Martin, D. Fried, Proc. SPIE 5725 (2005) 46.
[37] R.A. Bosch, O. Chubar, Am. Inst. Phys. Conf. Proc. 417 (1997) 35.
[38] Y.L. Matthis, P. Roy, B. Tremblay, A. Nucara, S. Lupi, P. Calvani, A. Gerschel, Phys. Rev. Lett. 80 (1998) 1220.
[39] P. Dumas, L.M. Miller, M.J. Tobin, Acta Phys. Pol., A 115 (2009) 446.
[40] G.L. Carr, O. Chubar, P. Dumas, in: I.W.L.R. Bahrgava (Editor), Spectrochemical Analysis Using Infrared Detectors, Blackwell Publishing, Oxford, UK, 2006.
[41] M. Pérez-Alonso, K. Castro, J.M. Madariaga, Curr. Anal. Chem. 2 (2006) 89.
[42] L. Miller, P. Dumas, Biochim. Biophys. Acta 1758 (2006) 846.
[43] G.D. Smith, J. Am. Inst. Conserv. 42 (2003) 399.
[44] J. Font, N. Salvadó, S. Butí, J. Enrich, Anal. Chim. Acta 598 (2007) 119.
[45] J. Bartoll, O. Hahn, U. Schade, Stud. Conserv. 53 (2008) 1.
[46] I. De Ryck, A. Adriaens, E. Pantos, F. Adams, Analyst (Cambridge, UK) 128 (2003) 1104.
[47] N. Salvadó, S. Butí, M.J. Tobin, E. Pantos, A.J.N.W. Prag, T. Pradell, Anal. Chem. 77 (2005) 3444.
[48] M. Cotte, E. Checroun, J. Susini, P. Walter, Appl. Phys. A89 (2007) 841.
[49] A. Lluveras, S. Boularand, J. Roqué, M. Coote, P. Giráldez, M. Vrendell-Saz, Appl. Phys. A 90 (2008) 23.
[50] M. Cotte, J. Susini, V. Armando-Solé, Y. Taniguchi, J. Chillida, E. Checroun, Ph. Walter, J. Anal. At. Spectrom. 23 (2008) 820.
[51] M. Cotte, P. Dumas, G. Richard, R. Breniaux, Ph. Walter, Anal. Chim. Acta 553 (2005) 105.
[52] V. Mazel, P. Richardin, D. Debois, D. Touboul, M. Cotte, A. Brunelle, Ph. Walter, O. Laprévote, Anal. Chem. 79 (2007) 9253.
[53] J.-P. Echard, M. Cotte, E. Dooryhee, L. Bertrand, Appl. Phys. A 92 (2008) 77.
[54] J.P. Echard, L. Bertrand, A. von Bohlen, A.S. Le Ho, C. Paris, L. Bellot-Gurlet, B. Soulier, A. Lattuati-Derieux, S. Thao, L. Robinet, B. Lavedrine, S. Vaiedelich, Angew. Chem., Int. Ed. Engl. 49 (2009) 197.
[55] I. Reiche, M. Lebon, C. Chadefaux, K. Müller, A.-S. Le H, M. Gensch, U. Schade, Anal. Bioanal. Chem., submitted for publication, 2010.
[56] M. Cotte, P. Walter, G. Tsoucaris, P. Dumas, Vib. Spectrosc. 38 (2005) 159.
[57] Y. Taniguchi, S. Aoki, Protecting the World Heritage Site of Bamiyan: Key Issues for the Establishment of a Comprehensive Management Plan 2004, Conservation Proposal, National Research Institute for Cultural Properties, Tokyo, Japan, 2004 pp. 76-90 (Chapter 6-2).
[58] Y. Taniguchi et al., Science for Conservation (in Japanese) 46 (2007) 181.
[59] Y. Taniguchi, H. Otake, M. Cotte, E. Checroun, Preprints 15th Triennial Meeting ICOM Committee Conserv., New Delhi, India, I (2008) 397-404.
[60] M. Cotte, P. Dumas, Y. Taniguchi, E. Checroun, P. Walter, J. Susini, Compte Rendu de Physique 10 (2009) 590.
[61] E. Stavitski, M.H.F. Kox, I. Swart, F.M.F. De Groot, B.M. Weckhuysen, Angew. Chem., Int. Ed. Engl. 47 (2008) 3543.
[62] G. Ellis, M.A. Gómez, C. Marco, J. Macromol. Sci., B Phys. 43 (2005) 191.
[63] F. Serrano, L. López, M. Jadraque, M. Koper, G. Ellis, P. Cano, M. Martín, L. Garrido, Biomaterials 28 (2007) 650.
[64] N. Kaun, S. Kulka, J. Frank, U. Schade, M.J. Vellekoop, M. Haraseke, B. Lendl, Analyst (Cambridge, UK) 131 (2006) 489.
[65] H.Y.N. Holman, D.L. Perry, M.C. Martin, G.M. Lamble, W.R. McKinney, J.C. Hunter-Cevera, Geomicrobiol. J. 16 (1999) 307.
[66] M. Schmidt, U. Schade, M. Grunze, Infrared Phys. Technol. 49 (2006) 69.
[67] M. Schmidt, N. Gierlinger, U. Schade, T. Rogge, M. Grunze, Biopolymers 83 (2006) 546.
[68] J.S. Lee, M. Schmidt, U. Schade, S.-W. Cheong, K.H. Kim, Phys. Rev. B 79 (2009) 073102.
[69] M. Schmidt, J.S. Lee, U. Schade, Infrared Phys. Technol. 53 (2010) 157.
[70] R. Bini, in: R.J. Hemley, G.L. Chiarotti, M. Bernasconi, L. Ulivi (Editors), Proc. Int. School Phys. ''Enrico Fermi'', Course CXLVII 2001, IOS Press, Amsterdam, The Netherlands, 2002.
[71] T.A. Strobel, M. Somayazulu, R.J. Hemley, Phys. Rev. Lett. 103 (2009) 065701.
[72] K. Grant, J. Ingrin, J.P. Lorand, P. Dumas, Contributions Mineral. Petrol. 154 (2007) 15.
[73] V.V. Struzhkin, A.F. Goncharov, R. Caracas, H.-K. Mao, R. Hemley, J. Phys. Rev. B. 77 (2009) 165133.
[74] C.T. Seagle, W. Zhang, D.L. Heinz, Z. Liu, Phys. Rev. B 79 (2009) 014104.
[75] E.M. Chamorro-Pérez, I. Daniel, J.C. Chervin, P. Dumas, J.D. Bass, T. Inoue, Phys. Chem. Mineral. 33 (2006) 502.

[76] R.J. Hemley, H. Mao, V.V. Struzhkin, J. Synchrotron. Radiat. 12 (2005) 135.
[77] E. Arcangeletti, L. Baldassare, D. Di Castro, S. Lupi, L. Malavasi, C. Marini, A. Perucchi, P. Postorino, Phys. Rev. Lett. 98 (2007) 196406.
[78] A. Perucchi, C. Marini, M. Valentini, P. Postorino, R. Sopracase, P. Dore, P. Hansmann, O. Jepsen, G. Sangiovanni, A. Toschi, K. Held, D. Topwal, D.D. Sarma, S. Lupi, Phys. Rev. B 80 (2009) 073101.
[79] M. Koch-Müller, S. Speziale, F. Deon, M. Mrosko, U. Schade, Phys. Chem. Mineral., submitted for publication, 2010.
[80] M. Mrosko, M. Koch-Müller, U. Schade, Jahrestagung der Deutschen Mineralogischen Gesellschaft 168 (2009) 87.
[81] L.-V. Moroz, M. Schmidt, U. Schade, T. Hiroi, M.A. Ivanova, Meteoritics Planet. Sci. 41 (2006) 1219.
[82] S.A. Sandford et al., Science for Conservation (in Japanese) 314 (2006) 1720.
[83] S. Bajt, S.A. Sandford, G.J. Flynn, G. Matrajt, C.J. Snead, A.J. Westphal, J.P. Bradley, Meteoritics Planet. Sci. 44 (2009) 471.
[84] F. Keilmann, Vib. Spectrosc. 29 (2002) 109.
[85] D. Vobornik, G. Margaritondo, J.S. Sanghera, P. Thielen, I.D. Aggarwal, B. Ivanov, N.H. Tolk, V. Manni, S. Grimaldi, A. Lisi, D.W. Piston, R. Generosi, M. Luce, P. Perfetti, A. Cricenti, J. Alloys Compd. 401 (2005) 80.